Strong Near-Field Enhancement of Radiative Heat Transfer between Metallic Surfaces

Tomas Kralik, Pavel Hanzelka, Martin Zobac, Vera Musilova, Tomas Fort, and Michal Horak

Institute of Scientific Instruments ASCR, v.v.i., Kralovopolska 147, 61264 Brno, Czech Republic

(Received 8 February 2012; published 27 November 2012)

Near-field heat transfer across a gap between plane-parallel tungsten layers *in vacuo* was studied experimentally with the temperature of the cold sample near 5 K and the temperature of the hot sample in the range 10–40 K as a function of the gap size d. At gaps smaller than one-third of the peak wavelength λ_m given by Wien's displacement law, the near-field effect was observed. In comparison with blackbody radiation, hundred times higher values of heat flux were achieved at $d \approx 1$ μm. Heat flux normalized to the radiative power transferred between black surfaces showed scaling $(\lambda_m/d)^n$, where $n \approx 2.6$. This Letter describes the results of experiment and a comparison with present theory over 4 orders of magnitude of heat flux.

DOI: 10.1103/PhysRevLett.109.224302 PACS numbers: 44.40.+a, 78.20.Ci

The first attempts to measure heat transfer between closely spaced bodies date from 1968–1973 [1,2], about 20 years after the first measurements of van der Waals forces between microscopically spaced bodies [3]. Both interactions have the same origin in electromagnetic near field due to thermally fluctuating dipoles.

A part of the electromagnetic waves originating or propagating within a body is transmitted through the surface and propagates into free space. Near the surface, the field of evanescent waves decays rapidly with the distance from the interface. When reaching over the opposite body, its energy can be transferred. The contribution of individual modes (magnetic or electric, s or p polarized) to the energy of this field depends on the type of interaction of electromagnetic field with matter (free or bound electrons) and varies with frequency and shows especially dramatic changes near the resonances (phonon-polariton in some dielectrics, plasmon polaritons in materials with free electrons) [4].

The near-field effect is expected at distances shorter than the wavelength of the peak of the blackbody emission. At room temperature the distance amounts to micrometers; whereas at low temperatures it may be tens of micrometers, which was the motivation of the cryogenic experiment of Domoto *et al.* [2].

In 1971, Polder and van Hove [5], prompted by Hargreaves's experiment [1], derived a complete and correct theoretical description of radiative heat transfer across a plane-parallel vacuum gap between nonmagnetic semi-infinite bodies, neglecting the effects of spatial dispersion. They utilized previous experience with the theory of van der Waals forces, in which thermal sources of the electromagnetic field were described using the fluctuation-dissipation theorem for fluctuating currents and were used as a field source in Maxwell's equations. The solution for the electromagnetic field, force interaction and heat transfer in plane-parallel geometries, can be then found by using the Green's functions formalism (for a review see Refs. [4,6,7]).

Polder and van Hove [5] analyzed the near-field effect for metallic surfaces and predicted energy transfer exceeding blackbody radiation. Comparison of their theory with Hargreaves's results was said to be problematic [5].

Much later, the interest in near-field effects, both thermally and optically generated, revived due to their importance in interactions between small objects and in the design of new types of microscopes (STM, AFM, NSOM), microelectromechanical, photovoltaic, and other new optical devices. In research of near-field heat transfer, specific problems were addressed—heat transfer at nanometric distances [8,9], effects of thermally excited resonant surface waves [4,6], effects of space dispersion [10], and theories for other specific geometries like dipole over plate surface [4], spheres [11], spheres and plates [12,13], films [6,14,15], general geometry [7,16], and the influence of roughness [17].

In contrast with the numerous theoretical studies, the experiments on the near-field effect on radiative heat transfer [1,8,18–21] offer only modest possibilities of comparison with the theory. They mostly span only 1 order of magnitude or less of heat fluxes [1] and are performed within a narrow interval of absolute temperatures [19–21], at single wavelength [18], or their geometry does not meet the demands of the present theory [8,19,20]. Recently, a room temperature experiment with plane-parallel geometry was published [21]. Within a span of 1 order of magnitude above far-field values, Ottens *et al.* [21] measured the heat transfer coefficient of the vacuum gap between sapphire samples and found good agreement with the theoretical results of Polder and van Hove [5]. Only two experiments were published previously for samples with metallic surfaces, one in plane-parallel geometry [1] and the other with a complicated geometry of a special STM tip above a planar sample [8]. In the STM experiment, the saturated heat flux region was reached at nanometric distances, where macroscopic electrodynamic theory gives diverging heat flux [5]. Heat fluxes within 3 orders of magnitude were measured by Kittel *et al.* [8].

In this Letter we present an experiment spanning 4 orders of magnitude of heat fluxes starting, in contrast to [8], at far-field values. Measurements were conducted with plane parallel samples, the temperature of the hot sample varying from 10 to 40 K. The results are compared with the theoretical prediction of heat flux across the vacuum gap d between metallic films on thick dielectric substrates. Supposing the temperatures T_2 and T_1 of the samples ($T_2 > T_1$), the relation for heat flux across the gap reads

$$q(T_1, T_2, d) = \int_0^\infty d\omega I(T_1, T_2, \omega) \int_0^\infty \frac{2\pi K dK}{(\omega/c)^2} \frac{1}{2}[\mathfrak{T}_\parallel + \mathfrak{T}_\perp],$$

where the integral of gap transmissivity is multiplied by the difference between spectral intensities of blackbody radiation at temperatures T_1 and T_2

$$I(T_1, T_2, \omega) = \frac{1}{\pi}\left(\frac{\omega}{2\pi c}\right)^2 \left[\frac{\hbar\omega}{\exp(\hbar\omega/k_B T_2) - 1} - \frac{\hbar\omega}{\exp(\hbar\omega/k_B T_1) - 1}\right]$$

and integrated over the frequencies ω. The wave vector component K parallel to the gap boundary is real valued and remains constant throughout the layered structure (Snell's law). Integration over all propagation angles within the vacuum gap (integration over $0 < K < \omega/c$), giving far-field contribution, is distinguished from the integration over $K > \omega/c$, corresponding to evanescent waves. Expressed in terms of Fresnel reflection coefficients $r_\perp^{(1)}$, $r_\parallel^{(1)}$, and $r_\perp^{(2)}$, $r_\parallel^{(2)}$ of the samples (at temperatures T_2 and T_1), respectively, the gap transmissivity $\mathfrak{T}_\perp^{\mathrm{FF}}$ for s-polarized radiation propagating between bodies reads [4,6,10]

$$\mathfrak{T}_\perp^{\mathrm{FF}} = \frac{(1 - |r_\perp^{(1)}|^2)(1 - |r_\perp^{(2)}|^2)}{|1 - r_\perp^{(1)} r_\perp^{(2)} \exp(2i\gamma_0 d)|^2}, \quad (1)$$

and similarly, the transmissivity for p-polarized waves. In this case, the surface perpendicular component of the wave vector *in vacuo*, $\gamma_0 = [(\omega/c)^2 - K^2]^{1/2}$, is a real number. Relation (1) is consistent with the well-known relation for radiative heat transfer between two surfaces based on Kirchhoff's law [4–6].

For $\omega/c < K < \infty$, $\gamma_0 = i\gamma_0''$ is a purely imaginary number and the gap transmissivity can be written in a form indicating exponential damping of evanescent waves *in vacuo* (near field, NF) with distance from the body surface

$$\mathfrak{T}_\perp^{\mathrm{NF}} = \frac{4\mathrm{Im}(r_\perp^{(1)})\mathrm{Im}(r_\perp^{(2)}) \exp(-2\gamma_0'' d)}{|1 - r_\perp^{(1)} r_\perp^{(2)} \exp(-2\gamma_0'' d)|^2},$$

and similarly, the transmissivity for p-polarized waves.

In the presented experiment identical samples with metallic films were used ($r_\perp^{(1)} = r_\perp^{(2)}$ and $r_\parallel^{(1)} = r_\parallel^{(2)}$). For the calculation of Fresnel reflection coefficients of samples we used the Drude model for tungsten permittivity

$$\varepsilon = \varepsilon_b - \frac{\omega_p^2}{\omega(\omega + i/\tau)}, \quad (2)$$

with plasma frequency $\omega_p = 9.73 \times 10^{15}$ s^{-1}, $\varepsilon_b = 1.07$ [22] and the relaxation time τ found by fitting to the measured data. Tungsten was selected for its nonmagnetic properties, hardness, and as a metal with normal skin effect. An Al_2O_3 ceramic (alumina), used as a substrate of the tungsten layers, was approximated by optical constants of sapphire [22] (measured values of far infrared reflectivity of used polished alumina samples are very close to those of sapphire). Numerical analyses for samples with thick substrates (> 10 μm) and reflective reverse sides showed that the results are only slightly sensitive to the substrate thickness and accurate values of optical constants of alumina. Disc substrates 2.5 mm thick and 35 mm in diameter were cut from alumina plates (ceramics Al_2O_3 of 99.8% purity and with density of 3.87 g/cm^3) and polished to a roughness lower than 0.1 μm. Pure alumina was chosen as an UHV compatible and solderable dielectric material with good shape stability and high thermal conductivity. A planarity of 0.6 and 0.1 μm of the two slightly concave samples was determined by HeNe laser interferometry. Small pits were found on the surface of the samples [23]. Tungsten layers 150 nm thick were sputtered on the polished substrates. This thickness was chosen to prevent peeling off, but to be at least comparable with the skin depth. The sputtered tungsten films have been characterized by room temperature resistivity $\rho(300\ \mathrm{K}) = 2.7 \times 10^{-7}\ \Omega\,\mathrm{m}$ measured with the four point probe and by the ratio between resistivity measured at 300 K and at the temperatures 77 and 4.2 K, $\rho(300\ \mathrm{K})/\rho(77\ \mathrm{K}) = \rho(300\ \mathrm{K})/\rho(4.2\ \mathrm{K}) = 1.40$. The constant resistivity $\rho_{\mathrm{res}} = 2 \times 10^{-7}\ \Omega\,\mathrm{m}$ of tungsten samples below 77 K has been derived from those electrical conductivity measurements, resulting in electron relaxation time $\tau_{\mathrm{EC}} = 6 \times 10^{-15}$ s. The emissivity of reverse sides and cylindrical sides of the samples was lowered by aluminization. Possible deformation of each sample due to the contractions mismatch during cooling was prevented by a thermal stress relieving mount (Fig. 1).

To examine experimental reproducibility, two runs of measurement were conducted, each one with the new cleaning and installation of the same samples. The samples were cleaned by washing and rinsing with submicron filtered water and dried by filtered gaseous nitrogen jet. Then they were put together face to face immediately after the cleaning process and installed in the measurement chamber of the apparatus described in detail in Ref. [24]. After the apparatus evacuation the samples were moved apart and then pumping continued for several hours.

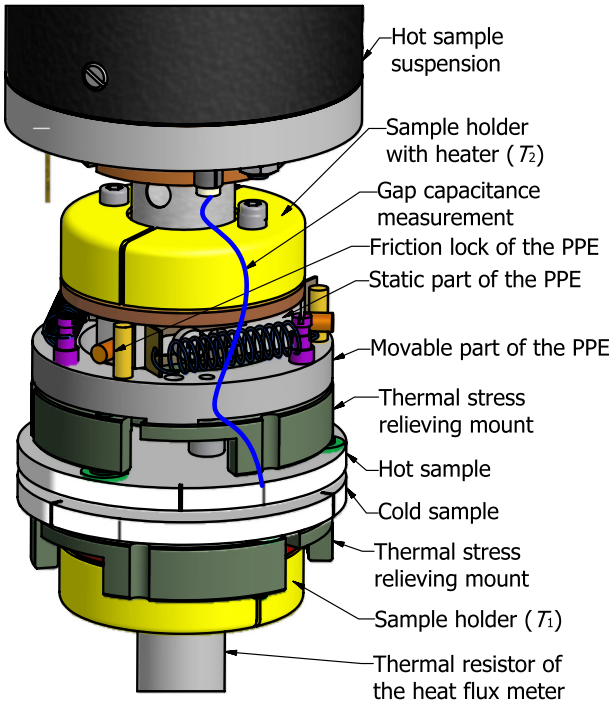

FIG. 1 (color online). Scheme of the central part of the measurement chamber containing samples with the plane-parallelism equalizer (PPE). Differential screw sets the positions of the static part of the PPE which is attached to the sample holder at the end of the sample suspension. The static and movable parts of PPE are coupled via three friction locks realized by three pairs of polished pins pressed against each other with a spring. When the sample suspension is shifted downwards until the contact between samples is achieved, and shifted further, the friction locks slip and plane parallelism between samples is set. Both parts of the PPE are thermally interconnected by a soft copper braid.

The whole apparatus was immersed in liquid helium which cools the measurement chamber below 5 K. Vacuum was maintained by cryopumping at a pressure lower than 10^{-8} Pa, reducing thus the heat transfer by molecular flow below measurable values.

After cooldown of the apparatus, the samples are set in plane-parallel position with zero gap (Fig. 1). Once plane parallelism was adjusted, the hot sample was moved up into the starting position about 200 μm above the cold sample. The zero gap was detected by disappearance of the electric contact between samples. Preservation of the plane-parallel position is ensured by two flexure membranes, part of hot sample suspension, that bear the sample holder in axial position [24].

The hot sample position was derived with a precision of 0.5 μm from the reading scale of the differential screw. The device enables us to set plane parallelism and distance between samples with an accuracy of $\sim$1 μm, which we deduce from the scatter of measured capacitance and transferred heat obtained after many independent parallelism adjustments following after breaking of parallelism during reset of the plane-parallelism equalizer, Fig. 1, [24].

Heat flow over the vacuum gap is absorbed by the cold sample and sinks into the liquid helium bath through a calibrated thermal resistor, serving as a heat flow meter. High temperature stability of the foot of the thermal resistor together with a resolution of 50 μK of the temperature measurement enabled us to measure heat flows from 20 nW to 1 mW.

Keeping the cold sample at $\approx$ 5 K, experimental results were obtained at varying distances d between surfaces at constant temperature T_2 of the hot sample (Fig. 2), and vice versa, with varying T_2 at constant d. All measured data are collected in Fig. 2 where the heat flux normalized to the blackbody emissive power, q/q_{BB}, $q_{BB} = \sigma_B(T_2^4 - T_1^4)$, is plotted as a function of $T_2 d$. The inset of Fig. 2 shows absolute values of measured heat fluxes obtained at $T_2 = 20$ K.

The near-field values, theoretical and experimental, follow approximately the same dependence (Fig. 2). We can observe the onset of the near-field effect at $T_2 d_0 \approx 1000$ K μm. Comparing it to the wavelength λ_m from Wien's displacement law, $T\lambda_m \approx 3000$ K μm, we get $d_0 \approx \lambda_m/3$ ($d_0 \approx$ 50 μm at $T_2 = 20$ K, for example).

Calculations of theoretical values were done for tungsten layers 150 nm thick characterized by permittivity

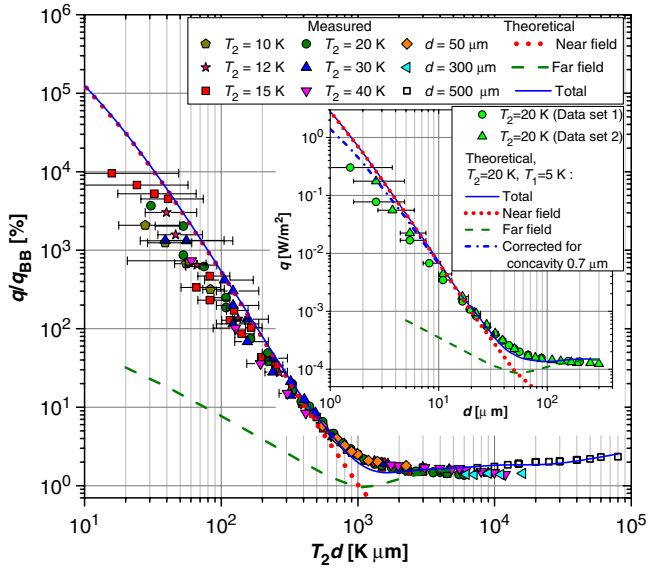

FIG. 2 (color online). Experimental and theoretical data on heat transfer over vacuum gap $d \approx$ 1–300 μm between samples with 150 nm thick tungsten layers on polished alumina substrate. Main graph: measured heat flux at temperatures $T_1 \approx 5$ K, $T_2 =$ 10–40 K, normalized to the heat flux $q_{BB} = \sigma_B(T_2^4 - T_1^4)$ transferred between black surfaces, is plotted as a function of the gap width ($d \approx$ 1–300 μm) and the temperature T_2 product. Theoretical values are calculated for $T_1 = 5$ K and $T_2 = 20$ K. Open squares are far field data ($d \approx 500$ μm, $T_2 =$ 15–160 K) derived from heat transfer measured between one of the samples and a black surface. Inset: Heat flux q measured at $T_2 = 20$ K and $T_1 = 5$ K versus gap d. Effect of samples concavity is shown by the lower curve at highest heat fluxes.

according to the Drude model, Eq. (2). As the theoretical curves $q/q_{BB} = f(T_2 d)$ coincide within $\pm 15\%$ when evaluated at various temperatures T_2 from 10 to 40 K they are represented by the results obtained for $T_2 = 20$ K in Fig. 2.

In the near-field regime, $T_2 d < 500$ K μm, the fit between theoretical and experimental data was achieved with the value $\tau_{NF} = 8 \times 10^{-15}$ s of relaxation time of Drude model, Eq. (2). This parameter is in reasonable agreement with the relaxation time obtained from dc measurement of electrical resistivity of tungsten layers of the samples, $\tau_{EC} = 6 \times 10^{-15}$ s. The difference between τ_{EC} and τ_{NF} may be attributed to the effective samples area reduction due to the isolated depressions formed by pits [23].

The near field spreads across the gap at long wavelengths, several times longer than the gap width. For example, numerical predictions of present experiment for 50 μm gap at 20 K ($T_2 d = 1000$ K μm) show that in the far field, most of energy ($> 75\%$) is radiated at wavelengths shorter than about 300 μm, whereas the spectrum of 75% of power transferred by the near-field interactions spans wavelengths longer than several millimetres. Unlike the far field, the near-field energy transferred between metals with plane parallel surfaces originates dominantly from s-polarized modes [10], i.e., modes with the electric field intensity parallel to the metal surface.

Open squares in Fig. 2 represent far-field experimental data derived from independent measurement of heat transferred between one of the samples and the black surface (measurement of sample emissivity). We can see good agreement with data measured between two opposite samples with the tungsten layer and values calculated from emissivity measurement (at higher values of d the effect of some leakage of radiation energy from the highly reflecting gap between metallic samples may be observed). Contrary to the near-field regime, the pits on the surface of the measured samples enhance the emission and absorption of heat radiation shortening thus the fitted relaxation time to the value $\tau_{FF} = 3 \times 10^{-15}$ s (fit to data in the far field region, $T_2 d > 2000$ K μm).

In the near-field regime, the experimental exponent $n \approx 2.5$ in the dependence $q/q_{BB} = q/\sigma_B(T_2^4 - T_1^4) \approx f(T_2\, d) \propto 1/d^n$ is lower than the theoretical one, $n \approx 2.7$. The experimental values could be influenced by the fact that we measure the least distance d between samples. In the case of deviation from the plane parallelism (slight concavity and possible sample inclination after gap zeroing) the measured value d is slightly less than the mean gap width. The last, according to Derjaguin's approximation [3,17], should be used in comparison between theory and experiment. Inset of Fig. 2 shows the effect of concavity of the samples which is equivalent to about 0.3 μm increase in the plane parallel gap. A further increase of up to 0.5 μm in the mean gap value may need to be added to the measured value because of the uncertainty in the zeroing (when zero gap is indicated a residual gap may be remaining with slightly inclined sample prospectively). The precision of reading of the final hot sample position is within 0.5 μm. Error bars in Fig. 2 visualize the total error in the mean gap values. Due to the method of measurement of transferred heat flux q, the temperature of cold sample increased above 5 K by few Kelvins at the highest values of q. Using theoretical dependencies, we can represent this effect with an equivalent increase in the vacuum gap between samples. Up to 0.5 μm was assessed for the highest heat fluxes measured at individual temperatures T_2.

In summary, we have observed near-field heat transfer over a vacuum gap between plane parallel tungsten layers characterized by a reflectivity of $\approx 97\%$. Heating one sample to temperatures from 10 to 40 K, substantially higher than the temperature of the cold sample kept at ≈ 5 K, we observed heat fluxes nearly 10 000 times increased above far-field values. This is 100 times higher than the heat flux between blackbodies according to the Planck's law.

The onset of near-field heat transfer was observed once the vacuum gap reached values lower than one-third of the wavelength λ_m given by Wien's displacement law for the thermal radiation of the hot sample.

Reasonable agreement between theoretical values and experimental data on near-field heat fluxes was achieved. Within more than 3 orders of magnitude above far-field values, both the experimental and theoretical data obtained at various temperatures of the hot sample from 10 to 40 K, and ~ 5 K of the cold one, showed similar behavior, which can be approximately characterized as follows. (i) Heat flux normalized to the blackbody emissive power varied approximately only with the product of the temperature of the hot sample and the gap width which is equivalent to the dependence on the ratio between wavelengths of thermal radiation and gap width, λ_m/d; (ii) near-field heat fluxes changed with varying gap as $1/d^n$, where $n \approx 2.5$–2.7.

The authors thank L. Skrbek and D. Schmoranzer for valuable suggestions, F. Münz for reflectivity measurements, and acknowledge financial support by the GAAV CR (Grant No. IAA100650804) and EC and MEYS CR (Project No. CZ.1.05/2.1.00/01.0017) and institutional support RVO:68081731.

[1] C. M. Hargreaves, Phys. Lett. **30A**, 491 (1969); Ph. D. thesis, University of Leiden, 1973.
[2] G. A. Domoto, R. F. Boehm, and C. L. Tien, J. Heat Transfer **92**, 412 (1970).
[3] B. V. Derjaguin, I. I. Abrikosova, and E. M. Lifshitz, Q. Rev. Chem. Soc. **10**, 295 (1956).
[4] K. Joulain, J.-P. Mulet, F. Marquier, R. Carminati, and J.-J. Greffet, Surf. Sci. Rep. **57**, 59 (2005).
[5] D. Polder and M. van Hove, Phys. Rev. B **4**, 3303 (1971).
[6] S. Basu, Z. M. Zhang, and C. J. Fu, Int. J. Energy Res. **33**, 1203 (2009); Z. M. Zhang, *Nano/Microscale Heat Transfer* (McGraw-Hill, New York, 2007), Chap. 10.

[7] A. I. Volokitin and B. N. J. Persson, Rev. Mod. Phys. **79**, 1291 (2007).
[8] A. Kittel, W. Müller-Hirsch, J. Parisi, S.-A. Biehs, D. Reddig, and M. Holthaus, Phys. Rev. Lett. **95**, 224301 (2005).
[9] A. I. Volokitin and B. N. J. Persson, Phys. Rev. B **69**, 045417 (2004).
[10] P. O. Chapuis, S. Volz, C. Henkel, K. Joulain, and J.-J. Greffet, Phys. Rev. B **77**, 035431 (2008).
[11] A. Narayanaswamy and G. Chen, Phys. Rev. B **77**, 075125 (2008).
[12] C. Otey and S. Fan, Phys. Rev. B **84**, 245431 (2011).
[13] M. Krüger, T. Emig, and M. Kardar, Phys. Rev. Lett. **106**, 210404 (2011).
[14] M. Francoeur, M. P. Mengüc and R. Vaillon, J. Phys. D **43**, 075501 (2010).
[15] S.-A. Biehs, Eur. Phys. J. B **58**, 423 (2007).
[16] R. Messina and M. Antezza, Phys. Rev. A **84**, 042102 (2011).
[17] S.-A. Biehs and J.-J. Greffet, Phys. Rev. B **82**, 245410 (2010).
[18] K. P. Gaikovich, A. N. Reznik, V. L. Vaks, and N. V. Yurasova, Phys. Rev. Lett. **88**, 104302 (2002).
[19] A. Narayanaswamy, S. Shen, and G. Chen, Phys. Rev. B **78**, 115303 (2008).
[20] E. Rousseau, A. Siria, G. Jourdan, S. Volz, F. Comin, J. Chevrier, and J.-J. Greffet, Nature Photon. **3**, 514 (2009).
[21] R. S. Ottens, V. Quetschke, S. Wise, A. A. Alemi, R. Lundock, G. Mueller, D. H. Reitze, D. B. Tanner, and B. F. Whiting, Phys. Rev. Lett. **107**, 014301 (2011).
[22] *Optical Constants of Solids*, edited by E. Palik (Academic, New York, 1991), and references therein.
[23] The pits of lateral dimension from $\sim$1 to $\sim$10 μm, small in comparison with the wavelengths of low temperature thermal radiation, cover about 10% of the sample area. At the narrowest gaps, we assume their effect on the transferred heat to be equivalent to the corresponding surface area reduction.
[24] T. Kralik, P. Hanzelka, V. Musilova, A. Srnka, and M. Zobac, Rev. Sci. Instrum. **82**, 055106 (2011).